PPPL-2051

UC20-B,D,F

I-12135

PPPL--2051

DE84 004302

TFTR INITIAL OPERATIONS

By

K.M. Young et al.

NOVEMBER 1983

MASTER

PLASMA PHYSICS LABORATORY

PRINCETON UNIVERSITY

PRINCETON, NEW JERSEY

PREPARED FOR THE U.S. DEPARTMENT OF ENERGY,
UNDER CONTRACT DE-AC02-76-CHO-3073.

TFTR INITIAL OPERATIONS

K.M. Young, M. Bell, W.R. Blanchard, N. Bretz, J. Cecchi,
J. Coonrod, S. Davis, H.F. Dylla, P.C. Efthimion, R. Fonck,
R. Goldston, D.J. Grove, R.J. Hawryluk, H. Hendel, K.W. Hill,
J. Isaacson, L.C. Johnson, R. Kaita, R.B. Krawchuk, R. Little,
M. McCarthy, D. McCune, K. McGuire, D. Meade, S.S. Medley,
D. Mikkelson, D. Mueller, E. Nieschmidt, D.K. Owens, A. Ramsey,
A.L. Roquemore, L. Samuelson, N. Sauthoff, J. Schivell, J.A. Schmidt,
S. Sesnic, J. Sinnis, J. Strachan, G.D. Tait, G. Taylor, F. Tenney,
and M. Ulrickson

Plasma Physics Laboratory, Princeton University
Princeton, New Jersey 08544, U.S.A.

ABSTRACT

The Tokamak Fusion Test Reactor (TFTR) has operated since December 1982 with ohmically heated plasmas. Routine operation with feedback control of plasma current, position, and density has been obtained for plasmas with $I_p \simeq$ 800 kA, a = 68 cm, R = 250 cm, and $B_t \simeq$ 27 kG. A maximum plasma current of 1 MA was achieved with $q \simeq 2.5$. Energy confinement times of ~ 150 msec were measured for hydrogen and deuterium plasmas with $\bar{n}_e \simeq 2 \times 10^{13}$ cm^{-3}, $T_e(0) \simeq$ 1.5 keV, $T_i(0) \simeq 1.5$ keV, and $Z_{eff} \simeq 3$. The preliminary results suggest a size-cubed scaling from PLT and are consistent with Alcator C scaling where $\tau \sim nR^2a$. Initial measurements of plasma disruption characteristics indicate current decay rates of ~ 800 kA in 8 ms which is within the TFTR design requirement of 3 MA in 3 ms.

I. INTRODUCTION

The Tokamak Fusion Test Reactor (TFTR), originally conceived in 1974, became operational in December 1982. This paper describes the experimental work in its first half year of operation; this work was carried on in parallel with major commissioning and testing of the various components of the tokamak.

The basic objectives of TFTR are i) to achieve temperatures (10 keV) and densities (10^{14} cm^{-3}) pertinent to a fusion reactor in plasmas with currents of 2.5 MA and ii) to achieve approximate energy break-even between the power input to and neutron power output from the plasma ($Q \sim 1$) at reactor-like fusion power densities (~ 1 W cm^{-3}). Both of these goals will be achieved with the addition of neutral beam heating power ($\sim$ 20 MW at 120 keV for $\sim$ 0.5 sec) and the latter goal with tritium plasmas. Within these goals, it is important to learn how to control high-current equilibria, to study confinement at high $n\tau_E$ of order 10^{13} cm^{-3} sec, where n is the electron density and τ_E the energy containment time, and to begin the study of the effects of α particles.

The neutral beamlines will be installed in the next two years, and in preparation for neutral injection it is essential to establish a good target ohmic plasma. The initial phase of these studies has been completed with emphasis on i) establishing 500-800 kA plasma currents, ii) evaluation of the operational range of density and associated energy containment, iii) evaluation of disruption characteristics, and iv) evaluation of discharge cleaning techniques. This phase is described here.

II. THE TFTR DEVICE

The major components of the tokamak, apart from the diagnostics, are shown in Fig. 1. For this operational period, the neutral beamlines and the igloo neutron shield were not in place.

The major operational parameters for TFTR are shown in Table 1. The limiting values of these parameters in this period are also compared with the goals of the TFTR program plan. The principal cause of the limitation on the magnetic field strengths has been the need to commission and test many rectifiers in their final circuit configurations and to use them with the tokamak only after very careful integrated tests.

In addition, a conservative small-radius carbon limiter configuration was used because of late delivery of the carbon-tile covered movable limiters and Inconel/stainless steel plates to cover the bellows sections of the vacuum vessel. The vertical dimension between the horizontal carbonplates of the limiter was 136 cm, the horizontal gap at the midplane was 150 cm. To provide additional protection of the bellows for plasmas collapsing inward, an additional stainless steel limiter plate at small major radius was provided ~ 180° toroidally around the tokamak. Under these circumstances, no significant studies of adiabatic plasma compression in major radius were possible, but testing of the feedback position control could be done.

A comparison of observed plasma currents is shown in Fig. 2 to show the progress made in improving the plasma since start-up. The design plasma current level of 2.5 MA is also shown.

Most of the experiments have been done using hydrogen plasmas, but a short study of deuterium plasmas was also done. The principal purposes were to get some preliminary data on the confinement of deuterium plasmas, and to allow a comparison of ion temperature measurement from the neutron flux and charge-exchange analyses.

The diagnostics for this operational period formed a subset of the final diagnostic set planned for TFTR.[1] This subset is listed in detail in Table 2. The table also includes estimates of the total number of data

channels and the number of raw data points collected by the Computer Instrumentation Control and Data Acquisition System (CICADA System) for the diagnostics for each plasma discharge. (This is about 60 percent of the total data handled in each discharge.)

III. VACUUM VESSEL CONDITIONING

The two principal techniques of conditioning the inside of the vacuum vessel and the components mounted inside it have been glow discharge cleaning and pulse discharge cleaning.[2] At the end of the operation period, the vessel was baked for about one day at ~ 100°C to test the vessel bakeout system.

Glow discharge cleaning was done by inserting two electrodes at ~ 400 V and running a 5 A glow discharge to the vessel wall. The glow was run almost continuously for about 100 hours after long periods of work inside the vessel in December and March, and then for periods of about eight hours each night between operational shifts whenever possible. Figure 3 shows the decay rates of CH_4 (16 amu) and CO and C_2H_4(28 amu) during the second cleaning period. H_2O (18 amu) fell to below background levels immediately. In total more than 100 equivalent monolayers of carbon and oxygen were removed in the two cleaning periods, and the resulting partial pressure of impurity gases was 1.5×10^{-8} Torr. For this cleaning, the vacuum vessel was not heated. Glow discharge cleaning has helped to clean some of the appendages to the vessel, particularly the large pumping ducts which cannot be cleaned by pulse discharge cleaning and presently cannot be baked.

However, glow discharge cleaning could not prepare the limiter adequately, and long periods of pulse discharge cleaning were necessary. A total of about 65 hours and 30,000 pulses were expended. A large fraction of the pulses were done at low hydrogen pressure, 2×10^{-5} Torr[3] with I_p ~ 200 kA

for ~100 msec duration and $B_T \sim 6$ kG with a repetition time of ~ 10 sec. This cleaning raised the limiter temperature (~ 200°C) and the vacuum vessel wall temperature and led to a significant production of CH_4, C_2H_4, and CO. A change to much higher pressure, 2×10^{-4} Torr[4] with $I_p \sim 80$ kA for ~ 50 msec duration at $B_T \sim 3$ kG, resulted in significant production of H_2O.

The combination of low and high fill pressure pulse discharge cleaning was certainly effective in conditioning the wall and limiter and led to the achievement of the long high plasma current discharges without disruptions. However, it is clear that much more cleaning is required since the impurity level in the plasma gives $Z_{eff} \gtrsim 3$, due mostly to carbon and oxygen impurities.

IV. PLASMA OPTIMIZATION

One of the principal goals during this operating phase has been to create and control high current discharges to allow effective confinement studies. Figure 2 shows the time behavior of the plasma current for some of these discharges. For the 1 MA plasma current case, q_{LIM} was 2.5 and in the highest density discharge achieved with 800 kA, the Murakami parameter ($n_e R/B_T$) was 2.3×10^{19} m^{-2} $T^{-1.5}$ The range of discharge conditions obtained in high current plasmas so far is shown in Fig. 4, where the inverse safety factor, 1/q, is plotted against the Murakami parameter. The total pulse length was about 2 sec and a constant current was maintained for ~ 0.8 sec for 800 kA and 600 kA discharges. The time scale for current buildup has been considerably longer than in previous machines operating under similar conditions. For example, the discharges begin to sawtooth at ~ 800 msec, compared to ~ 200 msec in PDX, and the sawtooth period is typically 25 msec compared to 5 msec. On the other hand, discharge initiation occurred rapidly

with a delay typically $\lesssim$ 1 msec over a wide range of parameters, despite eddy current induced fields which are especially large at breakdown.

The effectiveness of the feedback controls is demonstrated in Fig. 5. The time behaviors of the plasma current, voltage, horizontal position, and electron density are shown for an 800 kA deuterium discharge in a 2.7 T toroidal field. The plasma position and current are controlled by a hybrid digital/analog system consisting of an analog processor and a dedicated SEL 32/77 CICADA digital computer to control the power supplies.

The plasma position is measured by a set of 26 B_θ and B_ρ position coils mounted outside one of the bellows sections of the vacuum vessel. The individual coil signals are formed into weighted sums $\langle B_\theta \cos\theta \rangle$, $\langle B_\rho \sin\theta \rangle$, required to determine the position according to Shafranov's formula.[6] Extensive measurements of the vertical and radial magnetic fields, as a function of frequency, were taken inside the vacuum vessel prior to operation in order to allow the compensation of the Shafranov terms for stray fields due to eddy currents. An example from these measurements is shown in Fig. 6: a loop placed inside the vacuum vessel at its center was used to determine the vertical field as a function of the frequency applied to the ohmic heating coils.

The plasma current is measured by a Rogowski loop, which is also compensated for currents induced in the vacuum vessel. The plasma position and current control analog electronics compute the desired ohmic heating and equilibrium field coil voltages, which are converted by the computer into firing angles (i.e., the output voltage) of the OH and EF power supplies. Control is based on the difference between pre-programmed and measured I_p and I_pR. The system is fully programmable with time-varying gains, and with extensive computer control and monitor facilities. The power conversion

computer updates the power supply firing angles at a 1 kHz rate, the power supplies being effectively 24-pulse phase-controlled rectifiers operating off a 90-60 Hz supply.

During the initial TFTR experiments, control of quiescent discharges after start-up has been optimized to within 1% of the reference current and within a fraction of a centimeter of the reference position (Figs. 5a and 5c), without the use of feed-forward terms during the current flat-top.

The plasma's vertical position in TFTR is normally intrinsically stable. However, it has been found necessary to use a small preprogrammed radial field to correct minor field errors and so equalize heat loading on the upper and lower limiter blades.

Figure 5d shows the evolution of the line-averaged density. The density control system utilizes a CAMAC-based LSI 11/23 microcomputer as the control element. Data from fast, magnetically shielded ion gauges mounted on the torus, and from the double-pass 1 mm microwave interferometer viewing along a major radius, are digitized and processed along with preprogrammed reference waveforms to control the voltage applied to a fast piezoelectric valve. The nonlinear dependence of the flow on the voltage applied to the valve is corrected in software through use of a lookup table generated from prior calibration tests. A 500 Hz update rate is employed with simple proportional and feed-forward terms. Future enhancements to the system will include provisions for controlling multiple injection valves. At present, density feedback control is functional but limited in effectiveness by recycling and impurity influx from the walls and limiters.

Major components of TFTR have been designed to withstand the force associated with major disruptions in which the plasma current falls at the rate of 1 MA $msec^{-1}$. Among the approximately 300 well-controlled plasmas,

there have been about 50 major disruptions at plasma currents ranging from 200 kA to 950 kA. Forty of these disruptions have been well diagnosed. A histogram of the frequency of occurrence of disruptions within a band of current-fall rates is shown in Fig. 7. The fastest disruptions, one of which is shown in Fig. 8a, had a nearly constant fall rate of 100 kA $msec^{-1}$. This is well below the TFTR design value but is as fast as the measured major disruptions with beam heating on PDX.[7]

In every case, the major disruptions were preceded by a period of about 200 msec of minor disruptions or increased MHD activity. The progression of m=4,3,2 activity with a slowing down of the fluctuation frequency prior to the disruption has been detected by the Mirnov coils.

The distribution of fall rates indicates two types of disruption. The fast ones fell uniformly and were often preceded by minor disruptions. The slow ones fell in "stairsteps." They tended to occur when the plasma was dirty, indicated by increasing radiation prior to the disruption. In all cases, the plasma terminates on the inner wall: Fig. 8b shows this movement for the fast disruption of Fig. 8a.

V. PLASMA CONFINEMENT

Although the plasma major and minor radii have remained constant during this initial operational phase, some important confinement issues have been studied. The big increase in major and minor radius relative to other tokamaks operating in the last few years (PLT, PDX, DIII, Alcator C, ISX-B, TFR, T-10, FT, etc.) leads to a big increase in stored energy for the same densities and temperatures in ohmically heated plasmas. For example, TFTR has six times the volume of PLT. This increase in scale permits significant comparison of empirical scaling laws for energy confinement.

Initial operation of TFTR produced ohmically heated plasmas with $\bar{n}_e \sim 1\text{-}2.5 \times 10^{13}$ cm^{-3}, $T_e(0) \sim 1\text{-}2$ keV, $T_i(0) \sim 0.9\text{-}1.4$ keV, $B_T \sim 2.7$ T, and $I_p \sim 500\text{-}800$ kA with a current flat-top lasting about one second. Both hydrogen and deuterium plasmas were studied in detail. The characteristics of one deuterium discharge, shown in Fig. 5, will be reviewed in detail. During the current flat-top, the plasma voltage gradually approached 1 V, and both the line-integrated density and the central electron temperature (Fig. 9a) exhibited sawtooth-like fluctuations. The time evolution of the electron temperature 26 cm from the center (at R=220 cm, Fig. 9b) indicated a continuous broadening of the electron temperature profile during the plasma current flat-top. This increase in electron stored energy and simultaneous decreases in loop voltage resulted in an increase of the electron energy confinement time which reaches a maximum at about 1.4 seconds into the discharge. The electron temperature profile was parabolic squared in shape with a peak temperature ~ 1.5 keV. This temperature profile measured by a calibrated fast scanning radiometer was corroborated by the peak temperature measured by soft X-ray pulse-height-analysis.[8] The spectrum of the X-ray bremsstrahlung continuum is shown in Fig. 10; the slope corresponds to a temperature of 1.6 keV. Impurity K_α spectral lines of chlorine, iron, nickel, and chromium are also apparent, and their intensity can be used to estimate the heavy-ion contribution to Z_{eff}. The total Z_{eff} can be determined from the continuum intensity both in the X-ray and visible spectral regions. In this case, the total Z_{eff} is estimated to be 3.6 which is in the range 3-4 typical of this operation.

The ion temperature was obtained by charge-exchange measurement. Figure 11 shows the data for the ion temperature as a function of time, without including corrections of the data for opacity of the plasma. The ion

temperature at the center of the plasma was 1.4 keV--200 eV higher than the uncorrected data, as indicated by the one corrected point. In this deuterium discharge, the temperature could also be obtained from the neutron flux measured by a moderated He^3 proportional counter. The time evolution of the count rate is shown in Fig. 12. Assuming $Z_{eff} = 3$ to estimate the deuterium density, the temperature was calculated for a single time and is shown in Fig. 11 to be in good agreement with the charge-exchange result.

Total power efflux measured by the wide-angle bolometer during this discharge was about 60% of the input power; for the whole period of operation it ranged from 50 to 75% of the ohmic power. The assumption used in the analyses of the energy confinement time that the density profile was parabolic was confirmed from the unfolding of the visible bremsstrahlung emission from 6 radial chords assuming constant Z_{eff} profile and making use of the line-integrated density and electron temperature profile.

Confinement analyses were completed using the TRANSP time dependent transport-code.[9] This code calculates tokamak transport by analyzing the experimental data in terms of the one-dimensional magnetic field diffusion equation, evaluating the neutral density profile, and using particle and energy conservation equations. The total energy confinement time for this discharge was calculated to be $\tau_E \sim 170$ msec. The uncertainty in τ_E is estimated to be $\pm$ 20% based upon the accuracy of the density and temperature profile estimates. For similar electron densities in ungettered carbon limited discharges, the confinement time in PLT is between 25 and 50 msec.[10]

The total energy confinement times were calculated near the end of the current flat-top ($t \sim 1.4$ sec) where those times have reached their maximum values. In Fig. 13a the range of TFTR confinement time is included on the same plot of $\tau_E/\bar{n}$ vs. $R^{2.04}a^{1.04}$ utilized to infer the Alcator C confinement

scaling law from the published confinement times of many tokamaks.[11] On this plot, the TFTR confinement times agree with the predictions of the Alcator C scaling law. This R^2a dependence in confinement time scaling is similar to that proposed originally by Pfeiffer and Waltz.[12] Figure 13b is a linear plot of the TFTR total energy confinement times vs $\bar{n}$. Included are all of the well-documented discharges. These discharges vary in density over a range of $\bar{n} = 0.9 - 2.5 \times 10^{13}$ cm^{-3}. In addition, the predictions of the Intor, Alcator A ,[13] and Alcator C scaling laws are plotted. The TFTR confinement times clearly agree with the predictions of the Alcator C scaling of $\tau_E = 0.192\ \bar{n}\ R^{2.04}a^{1.04}$ (MKS units).

A total energy confinement time of 190 ms represents our best result. Note that the density range of comparison is only $\bar{n}=0.9 - 2.5 \times 10^{13}$cm^{-3}, a range insufficient to observe the saturation of confinement with density observed on many tokamaks. Furthermore, the present limitation of a fixed limiter position prevents us from directly observing any size scaling at this time. Experiments with variable limiter size and plasma position to determine size scaling in TFTR will commence this fall.

VI. CONCLUSIONS

The TFTR tokamak has operated very successfully over this initial period of operation and has already given important new information on confinement, control, and disruptions. Breakdown has been relatively easy over a very wide range of plasma parameters. The feedback control systems have worked well in holding the plasma fixed in position and in holding the plasma current and density constant for times up to 1 second. The containment times are larger than have previously been observed for ohmic plasmas, in the range from 130 to 190 msec. The next series of experiments with a movable

limiter will be aimed at a thorough evaluation of size scaling in ohmically heated plasmas.

The measured disruption decay scale of ~ 100 kA msec^{-1} is well within the mechanical design limit of TFTR. While a fully cleaned vacuum vessel has not yet been achieved and the plasmas have had Z_{eff} about 3, there is good evidence of successful cleanup with glow and pulsed discharge cleaning. With bakeout and further cleaning, lower Z_{eff} plasmas can be expected.

ACKNOWLEDGMENTS

Even more than usual, we owe our thanks to the very many engineers, computer programmers, and technicians who have worked with dedication for long and awkward hours to make this series of experiments happen. We also thank M.B. Gottlieb for his major role in initiating the TFTR Project and P.J. Reardon for his leadership throughout the construction phase. The construction was managed by a group from our major subcontractor, Ebasco, under J. French. We are grateful to H.P. Furth, P. Rutherford, and J.R. Thompson for their continued leadership, advice, and support. The staff of the U.S. Department of Energy has constantly supported the TFTR Project, and we are pleased to acknowledge that this work was done under U.S. Department of Energy Contract No. AC02-76-CHO-3073.

REFERENCES

[1]Johnson, L.C., and Young, K.M., in Proceedings of the Course on Diagnostics for Fusion Reactor Conditions, Varenna, Italy, 1982, Report EUR-8351-1EN.

[2]Dylla, H.F., Blanchard, W.R., Krawchuk, R.B., and Hawryluk, R.J. J. Vac. Sci. Technol. (to be published).

[3]Dylla, H.F., Bol, K., Cohen, S.A., Hawryluk, R.J., Meservey, R.B., and Rossnagel, S.M. J. Vac. Sci. Technol. 16, 752 (1979).

[4]Oren, L., and Taylor, R.J., Nucl. Fusion, 17, 1143 (1977).

[5]Murakami, M., Callen, J.D., and Berry, L.A., Nucl. Fusion 16, 347 (1976).

[6]Mukhovatov, V.S., and Shafranov, V.D., Nucl. Fusion, 11, 605 (1971).

[7]McGuire, K., Buchenauer, D., Couture, P., Izzo, R., Kawahata, K., Monticello, D., Okama, K., and Sauthoff, N., in Proceedings of the Symposium on Energy Removal and Particle Control in Toroidal Fusion Devices, Princeton, NJ, 1983.

[8]von Goeler, S., Hill, K.W., Bitter, M., Clifford, C., Fredd, E., Goldman, M., Johnson, L.C., Ku, L-P., Moshey, E., Renda, G., Sauthoff, N., Sesnic, S., Tenney, F., and Young, K.M., in Proceedings of the Course on Diagnostics for Fusion Reactor Conditions, Varenna, Italy, 1982, Report EUR-8351-1EN, Vol. 1, p. 69.

[9]Hawryluk, R.J., in Proceedings of the Course on Physics Close to Thermonuclear Conditions, Varenna, Italy, 1980, Report EUR RU/XIII/476.

[10]K. Bol, Arunasalam, V., Bitter, M., Boyd, D., Brau, K., Bretz, N., Bussac, J., Cohen, S., Colestock, P., Davis, S., Dimock, D., Dylla, H.F., Eames, D., Efthimion, P., Eubank, H., Goldston, R.J., Hawryluk, R.J., Hill, K.W., Hinnov, E., Hosea, J., Hsuan, H., Jobes, F., Johnson, D., Mazzucato, E., Medley, S., Meservey, E., Sauthoff, N., Schmidt, G., Stauffer, F., Stodiek, W., Strachan, J., Suckewer, S., Tait, G., Ulrickson, M., and von Goeler, S. in Plasma Physics and Controlled Nuclear Fusion Research (IAEA, Vienna, 1979), Vol. 1, p. 11.

[11]Alcator Group, in Plasma Physics and Controlled Nuclear Fusion Research IAEA, Vienna, in press) Vol. 1.

[12]Pfeiffer, W., and Waltz, R.E., Nucl. Fusion, 19, 51 (1979).

[13]Gondhalekar, A., Granetz, R., Gwinn, D., Hutchinson, I., Kusse, B., Marmar, E., Overskei, D., Pappas, D., Parker, R.R., Pickrell, M., Rice, J., Scaturro, L., Schuss, J., West, J., Wolfe S., Petrasso, R., Slusher, R.E., and Surko, S.M., in Plasma Physics and Controlled Nuclear Fusion Research (IAEA, Vienna, 1979), Vol. 1, p. 199.

TABLE 1: TFTR PARAMETERS

PLASMA	JUNE 1983	AUGUST 1984	APRIL 1986
Minor Radius a(cm)	68	85	85
Major Radius R(cm)	250	248	248
Toroidal Magnetic Field B_T(T)	2.7	4.0	5.2
Vertical Field from Equilibrium Field Coils (T)	0.19	0.3	0.42
Plasma Current I_p (MA)	1.0	1.5	2.5
Plasma Density n_e (cm^{-3})	2.5×10^{13}	5×10^{13}	5×10^{13}
Total Neutral Beam Heating Power (MW)	--	~ 10	~ 27
COIL AND ENERGY CONVERSION SYSTEM CAPABILITY			
Current in Ohmic Heating Coils I_{OH} (kA)	24	24	24
Volt-second capability ϕ_{OH} (V-sec)	6.5	12.5	12.5
Current in Equilibrium Field Coils I_{EF} (kA)	15	24	36
Open Circuit OH Rectifier Voltage (kV)	10	18	18
Open Circuit EF Rectifier Voltage (kV)	8	16	16
Capacitor Bank (MJ)	3.4	12	12
Available Energy from Motor Generator (MJ)	1350	2250	4500
Pulsed Power from Motor Generators (MVA)	475	475	950

TABLE 2: DIAGNOSTICS FOR INITIAL OPERATION

DIAGNOSTIC	MEASUREMENT	NO. OF DATA CHANNELS	RAW DATA POINTS
1 mm μWave Interferometer†	$\int n_e \, dl$	2	32 K
Torus Pressure Gauges†	Torus Pressure	2	8 K
Residual Gas Analysis	Gas Impurity Concentration	2	---
Rogowski Loops†	I_p	4	32 K
Position Coils†	Plasma Position	37	108 K
Mirnov Coils	Magnetic Oscillations	43	195 K
Voltage Loops/Saddle Coils	Voltage Around Torus, Position	44	88 K
Diamagnetic Loop	Plasma Pressure	4	4 K
Hard X-ray Monitors	Effects Of Runaway Electrons	5	40 K
Plasma TV	Plasma Pictures, Position	1	---
Fast Scan. Het. Radiometer	T_e (r,t)	2	32 K
X-ray Pulse-Height Analyzer	$T_e(t)$, n_{Fe}, Z_{eff}	9	102 K
Horizontal Charge Exchange	$T_i(t)$	198	198 K
U^{235}, BF_3, He^3 Neutron Proportional Counters	Runaway-Created Neutrons, $T_i(t)$	12	44 K
Bolometers	Radiated (and C-EX) Power	34	34 K
UV Survey Spectrometer	Impurity Spectrum (t)	2	64 K
Interference Filter Array	$Z_{eff}(t)$, H_ω light (t), $n_e(r,t)$	64	16 K
		465	997 K

†Participates in Feedback Control

FIGURE CAPTIONS

FIG. 1 An artist's impression of TFTR. The main components of the tokamak are identified.

FIG. 2 Plasma currents as a function of time. The small, short pulse of the first plasma and the planned 2.5 MA current are also shown.

FIG. 3 Dependence of the impurity partial pressures produced during the second glow discharge cleaning period (March-April 1983).

FIG. 4 The range of operating parameters during current flat-top for many discharges, both hydrogen and deuterium. The axes are the inverse safety factor and the Murakami parameter.

FIG. 5 The time dependence of a) plasma current, b) loop and surface voltage, c) plasma major radius, and d) line integrated density for one deuterium discharge.

FIG. 6 The measured effective vertical field components at the center of the vacuum vessel as a function of the frequency of applied voltage to the ohmic heating coils.

FIG. 7 Histogram of the number of disruptions in intervals of rate of fall of plasma current. Forty disruptions were analyzed.

FIG. 8 An example of a fast disruption. a) Time dependence of the current, and b) time dependence of the plasma position during the disruption.

FIG. 9 Time evolution of the electron temperature measured by the fast scanning heterodyne radiometer, a) at the center of the plasma, and b) 26 cm from the center.

FIG. 10 The soft X-ray pulse height analysis spectrum shows impurity K_α lines, with the bremsstrahlung giving a temperature of 1.64 keV.

FIG. 11 The ion temperature as a function of time from the charge-exchange system. One point is shown corrected for opacity. The ion temperature inferred from the neutron flux is also shown.

FIG. 12 Time dependence of the neutron flux measured by a moderated He^3 proportional counter.

FIG. 13a) TFTR confinement data superimposed on previously published data prepared by the Alcator Group for ohmically heated plasmas in many tokamaks.

FIG. 13b) The total energy confinement time as a function of average density for well-documented TFTR discharges. The predictions from three proposed scaling laws are also shown.

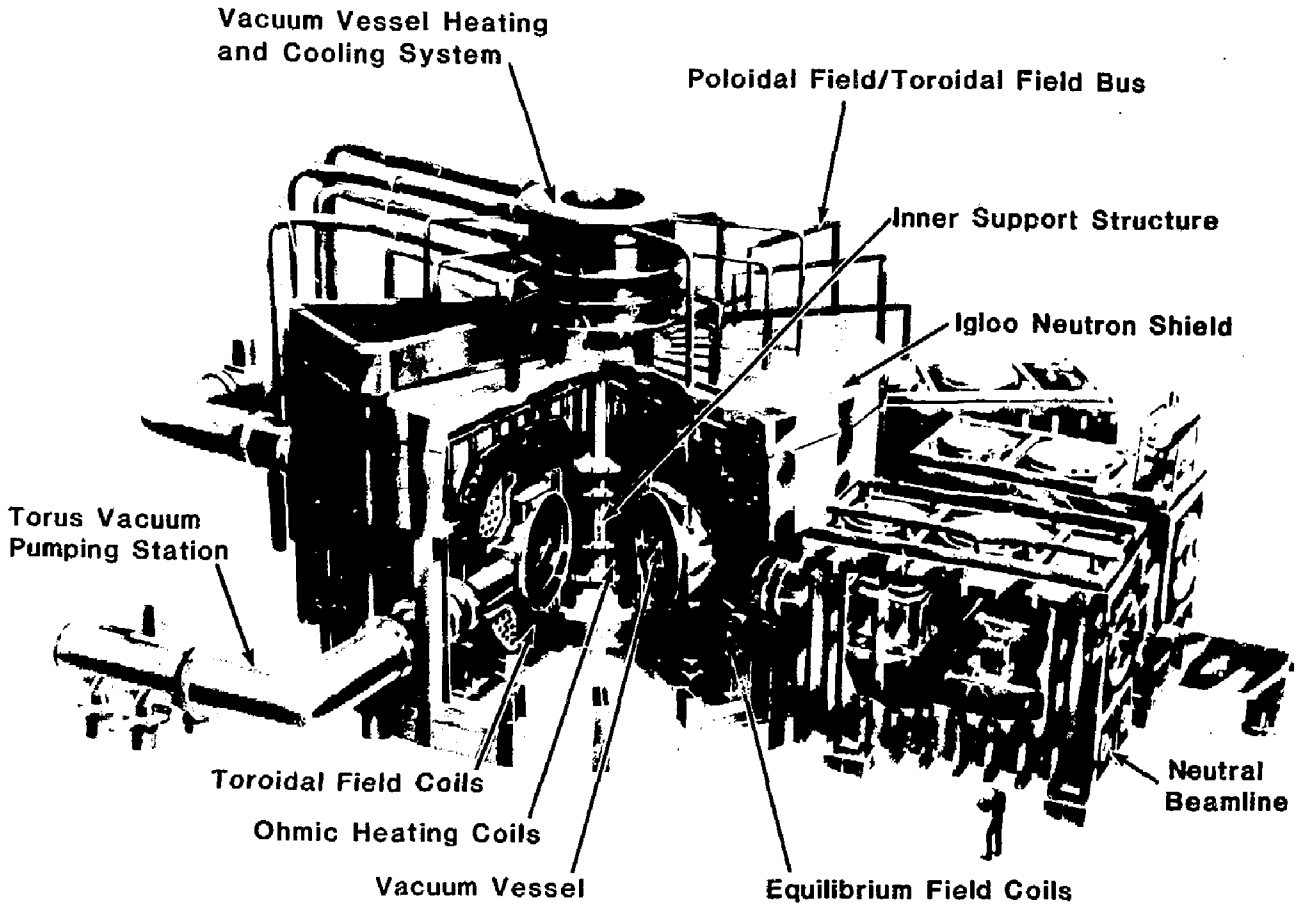
Vacuum Vessel Heating
and Cooling System
Poloidal Field/Toroidal Field Bus
Inner Support Structure
Igloo Neutron Shield
Torus Vacuum
Pumping Station
Toroidal Field Coils
Ohmic Heating Coils
Vacuum Vessel
Equilibrium Field Coils
Neutral
Beamline

Fig. 1

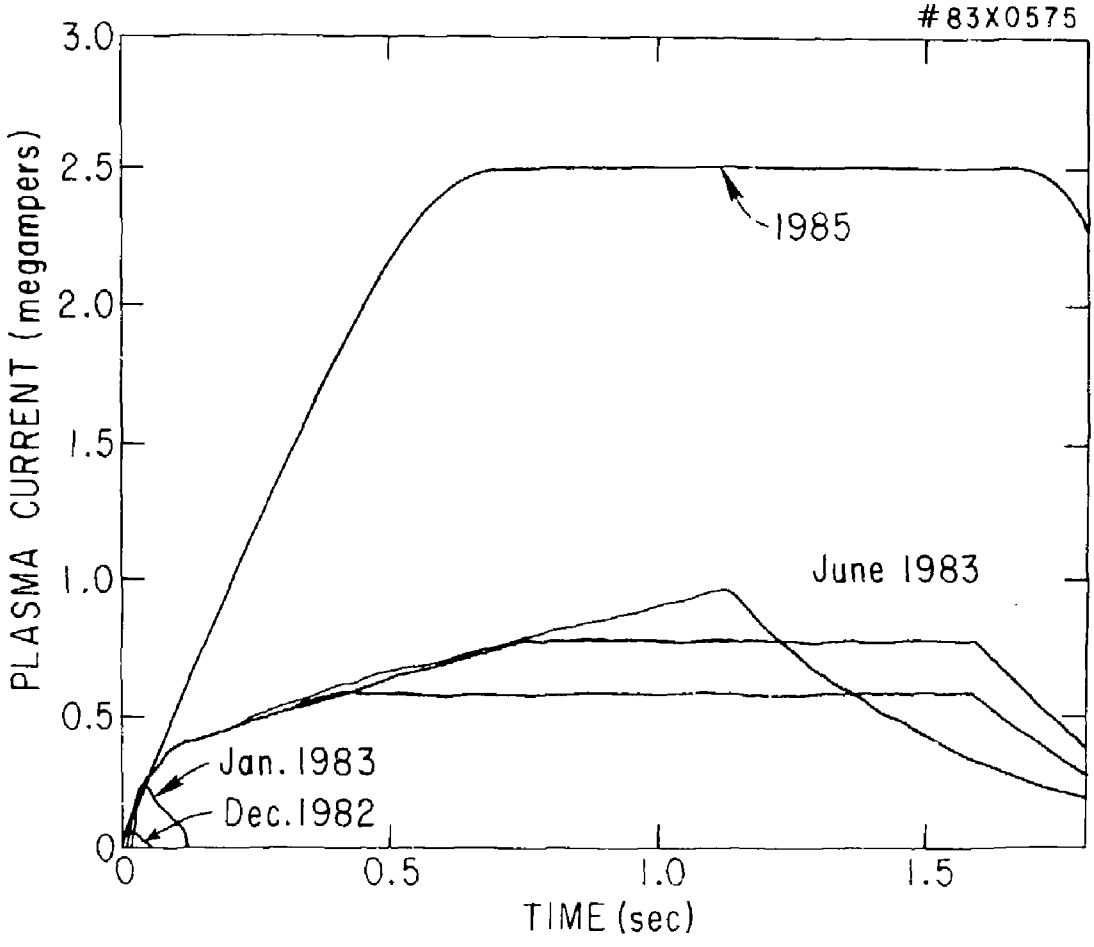
#83X0575
PLASMA CURRENT (megampers)
TIME (sec)
3.0
2.5
2.0
1.5
1.0
0.5
0
0
0.5
1.0
1.5
1985
June 1983
Jan. 1983
Dec.1982

Fig. 2

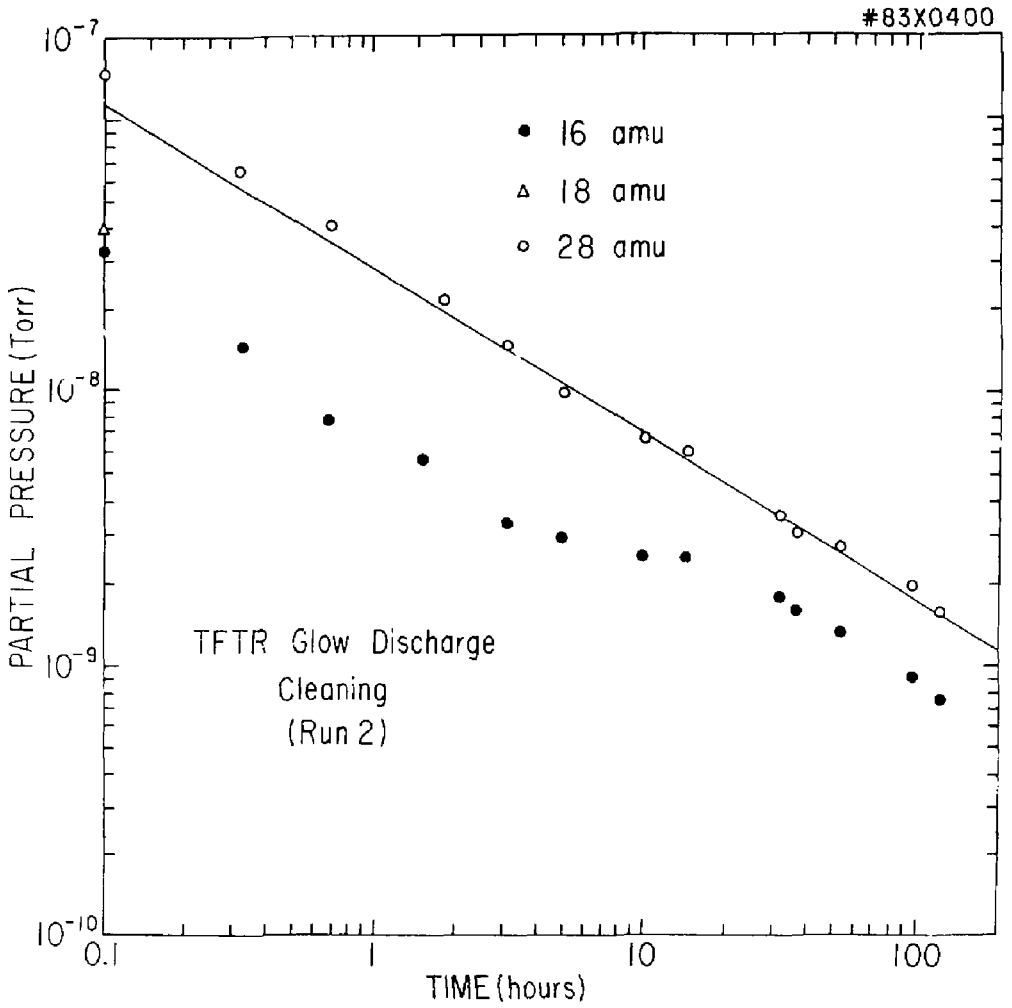
#83X0400
16 amu
18 amu
28 amu
TFTR Glow Discharge
Cleaning
(Run 2)
PARTIAL PRESSURE (Torr)
TIME (hours)
10^{-7}
10^{-8}
10^{-9}
10^{-10}
0.1
1
10
100

Fig. 3

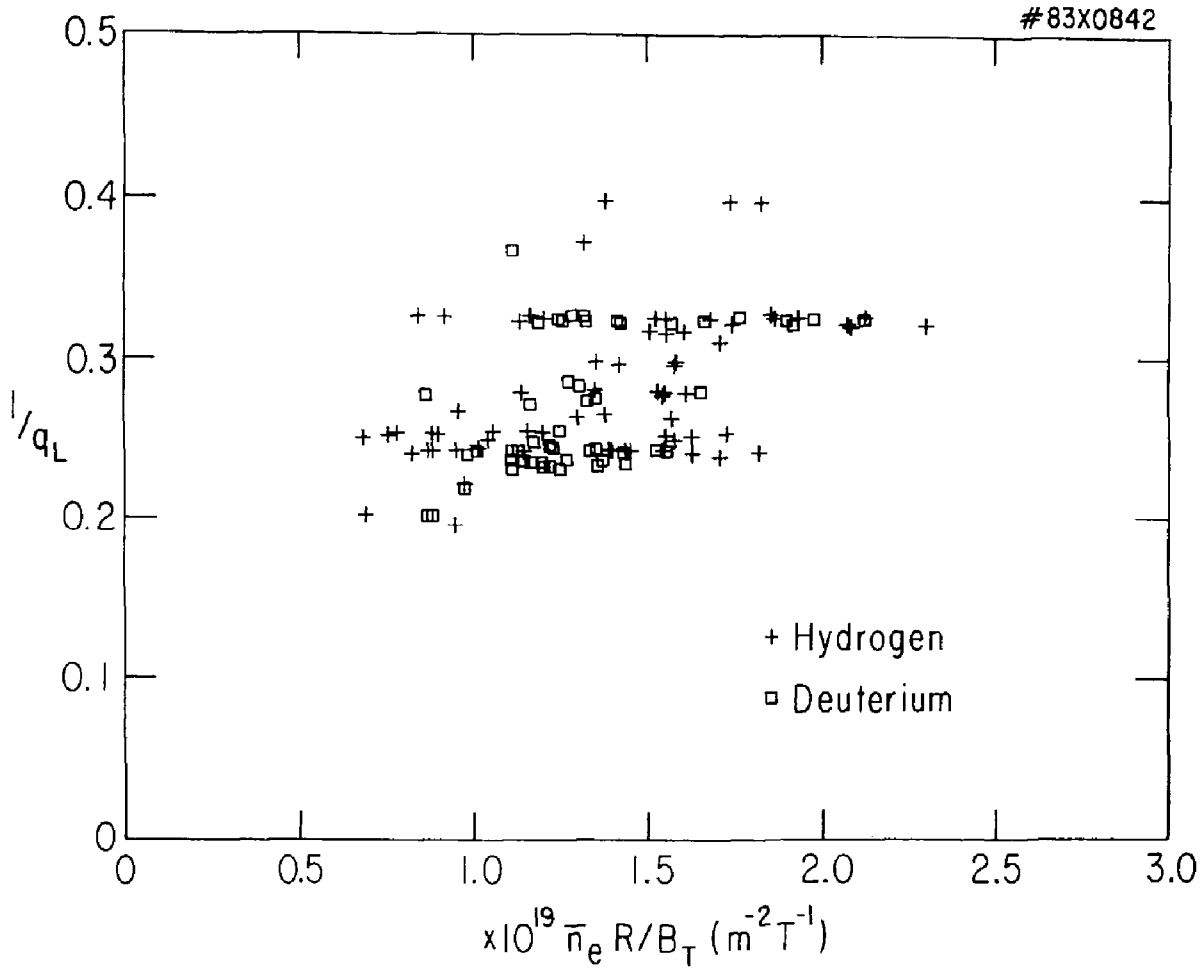
#83X0842
0.5
0.4
0.3
0.2
0.1
0
$1/q_L$
+ Hydrogen
□ Deuterium
0
0.5
1.0
1.5
2.0
2.5
3.0
$\times 10^{19} \bar{n}_e R/B_T$ ($m^{-2}T^{-1}$)

Fig. 4

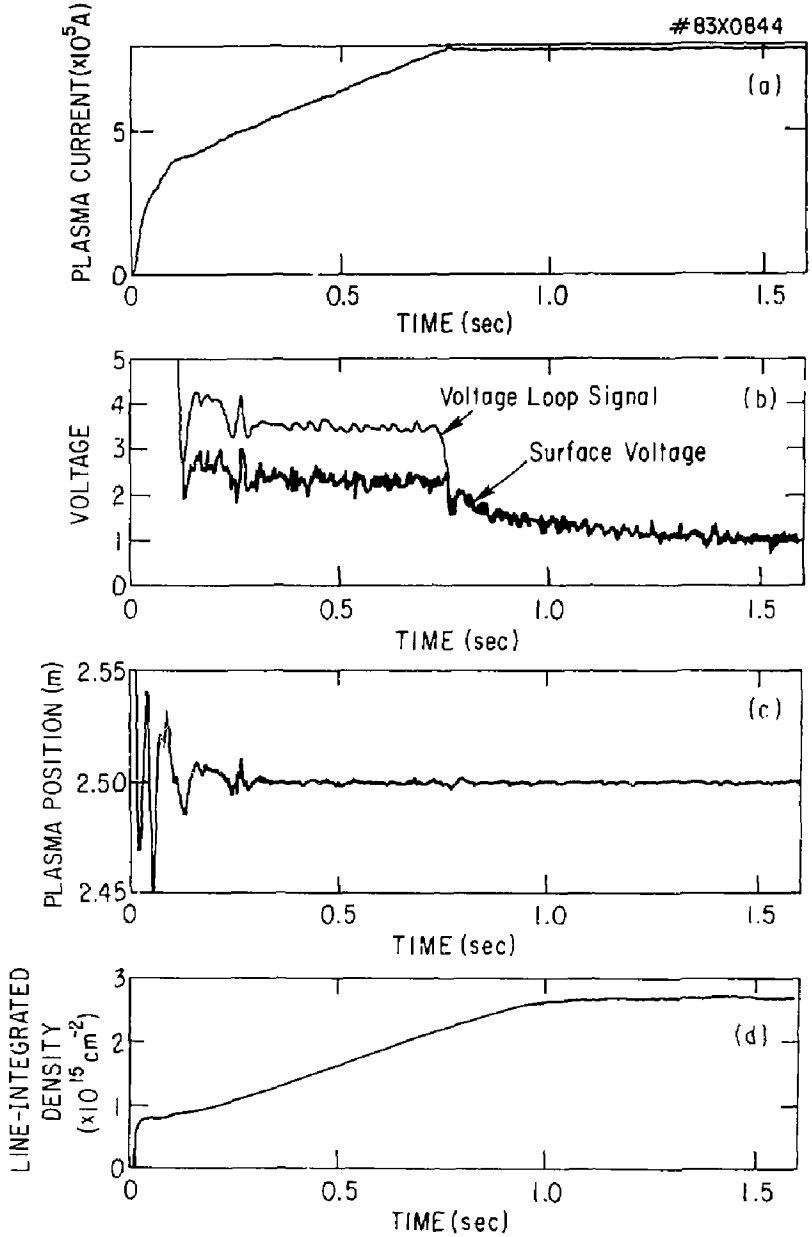
#83X0844
(a)
PLASMA CURRENT(x10^5A)
5
0
0
0.5
1.0
1.5
TIME (sec)
(b)
Voltage Loop Signal
Surface Voltage
VOLTAGE
5
4
3
2
1
0
0
0.5
1.0
1.5
TIME (sec)
(c)
PLASMA POSITION (m)
2.55
2.50
2.45
0
0.5
1.0
1.5
TIME (sec)
(d)
LINE-INTEGRATED DENSITY (x10^15 cm^-2)
3
2
1
0
0
0.5
1.0
1.5
TIME (sec)

Fig. 5

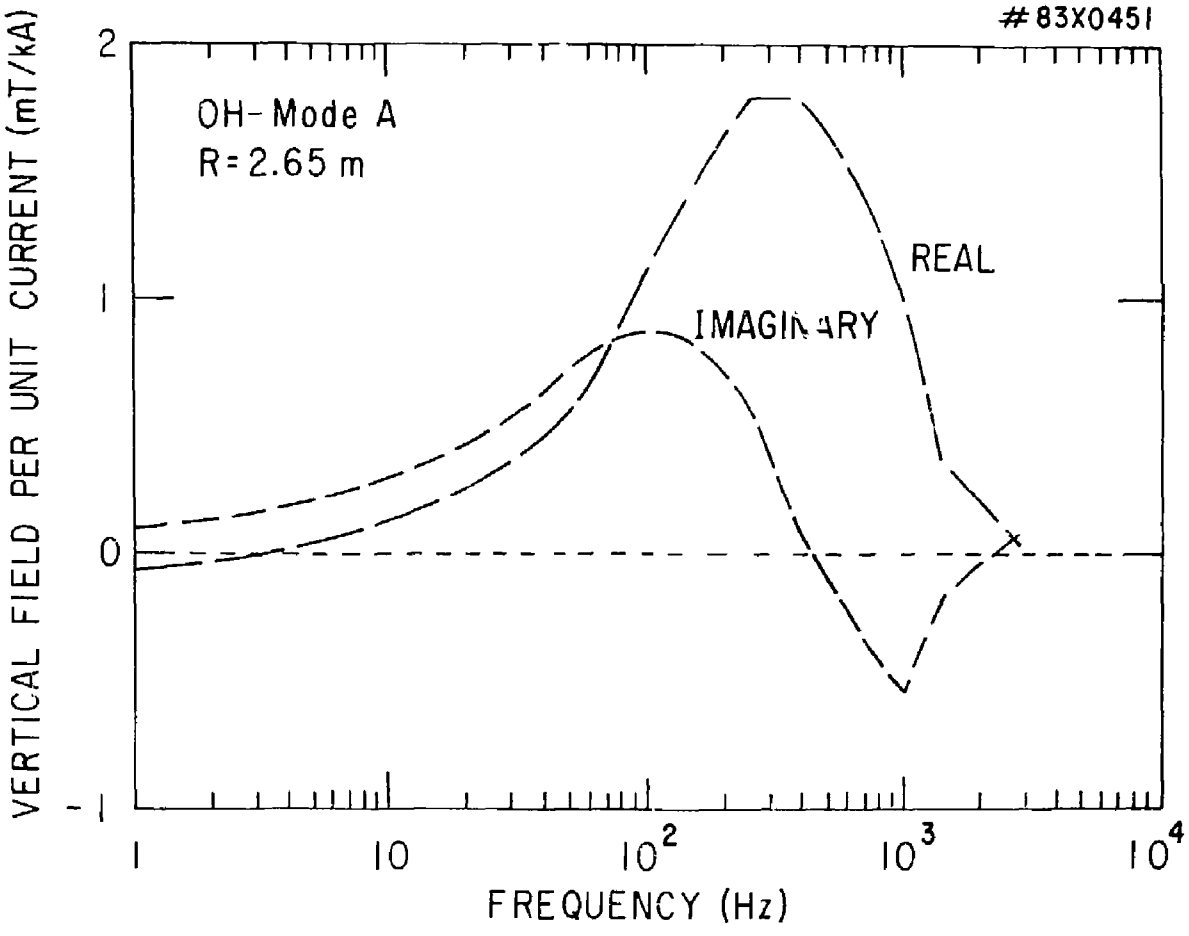
#83X0451
OH-Mode A
R=2.65 m
REAL
IMAGINARY
VERTICAL FIELD PER UNIT CURRENT (mT/kA)
2
1
0
-1
1
10
10^2
10^3
10^4
FREQUENCY (Hz)

Fig. 6

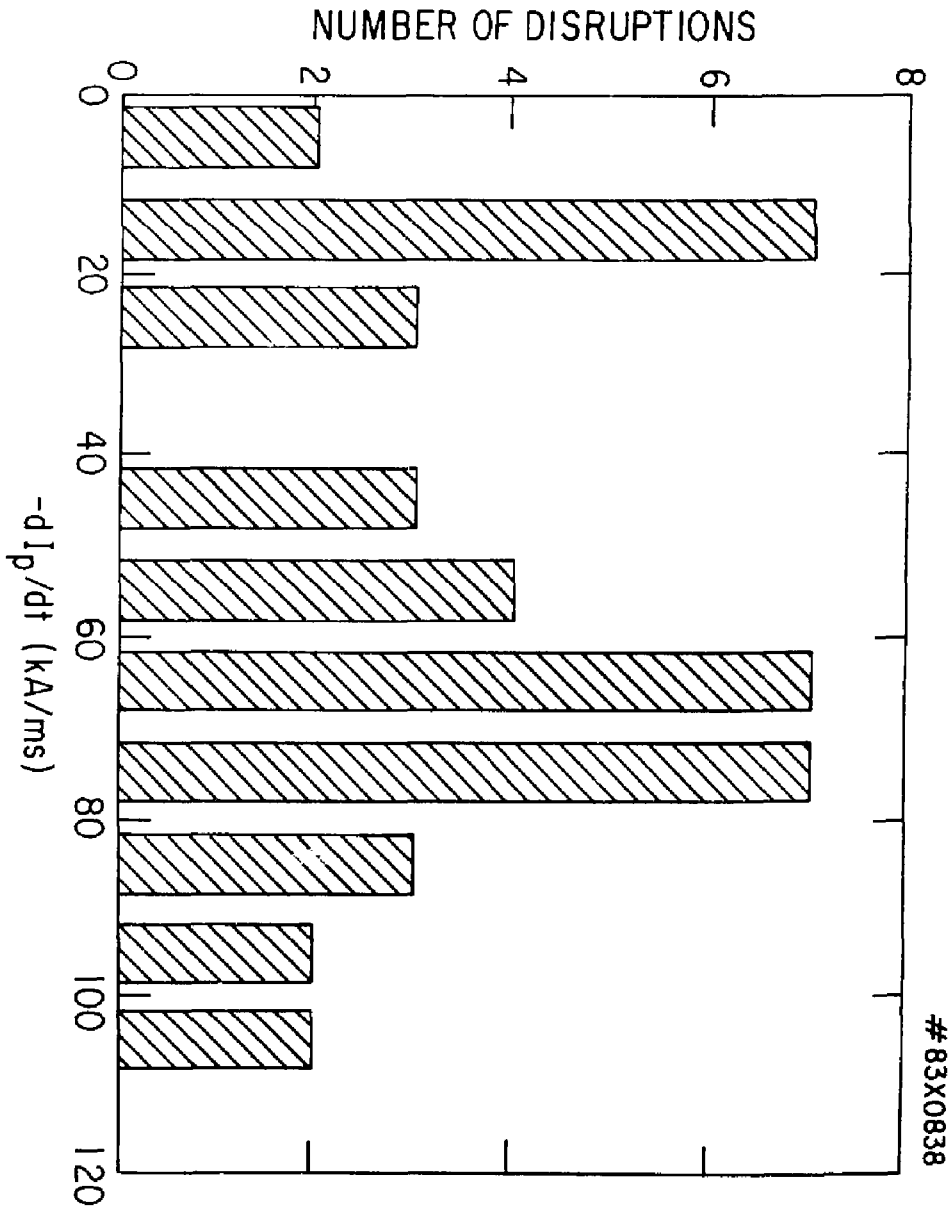
NUMBER OF DISRUPTIONS
0
2
4
6
8
0
20
40
60
80
100
120
-d I_p/dt (kA/ms)
#83X0838

Fig. 7

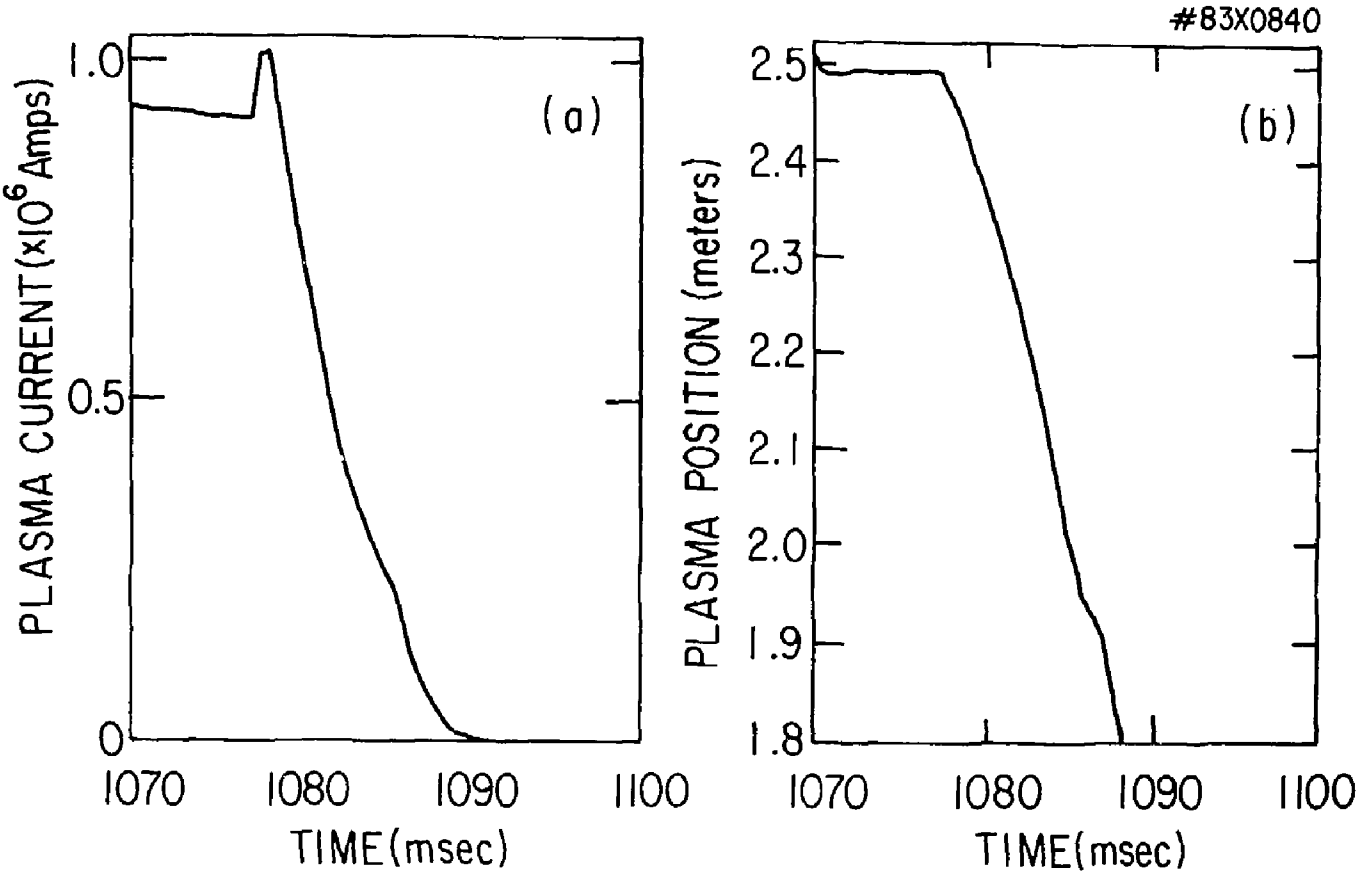
#83X0840
PLASMA CURRENT (x10^6 Amps)
1.0
0.5
0
(a)
1070
1080
1090
1100
TIME(msec)
PLASMA POSITION (meters)
2.5
2.4
2.3
2.2
2.1
2.0
1.9
1.8
(b)
1070
1080
1090
1100
TIME(msec)

Fig. 8

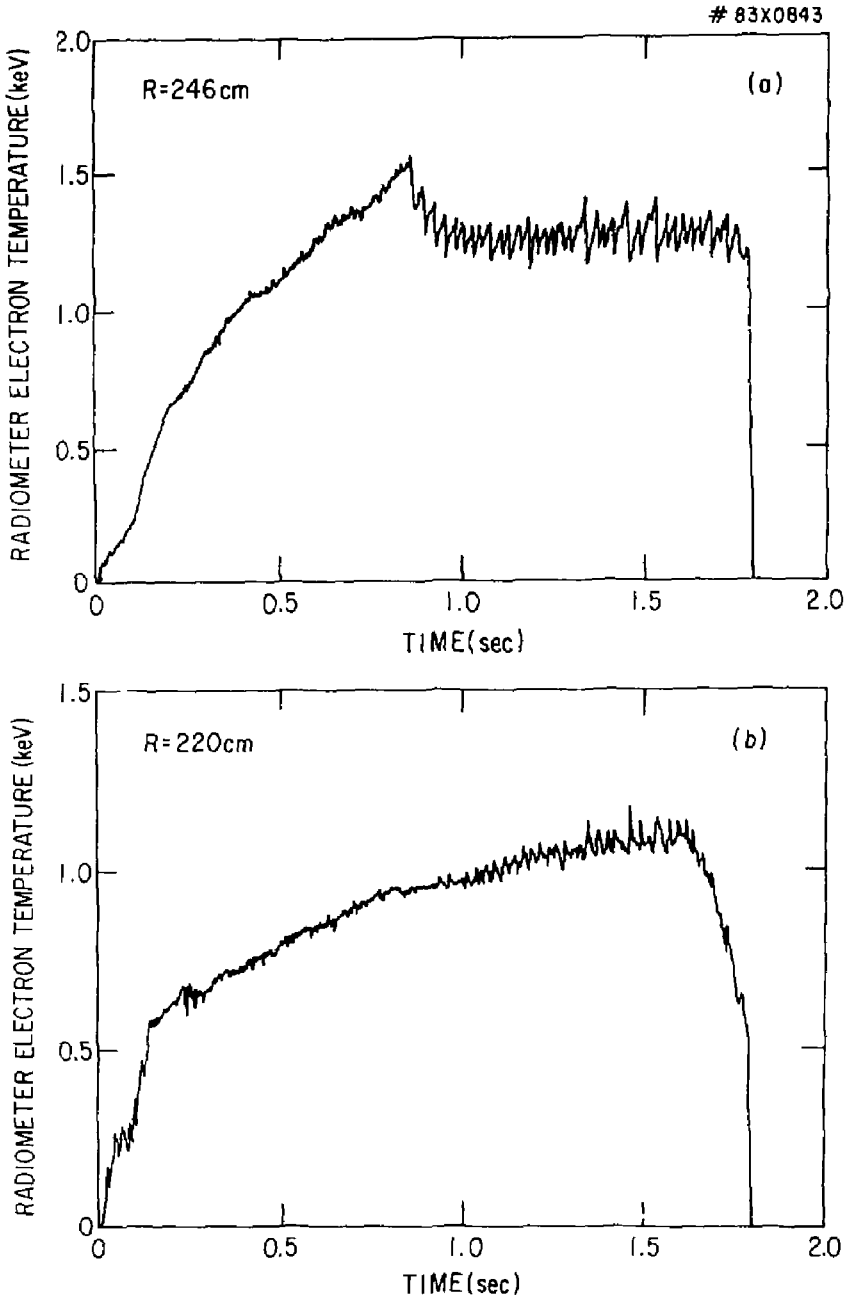
# 83X0843
R=246cm
(a)
RADIOMETER ELECTRON TEMPERATURE(keV)
TIME(sec)
R=220cm
(b)
RADIOMETER ELECTRON TEMPERATURE (keV)
TIME(sec)

Fig. 9

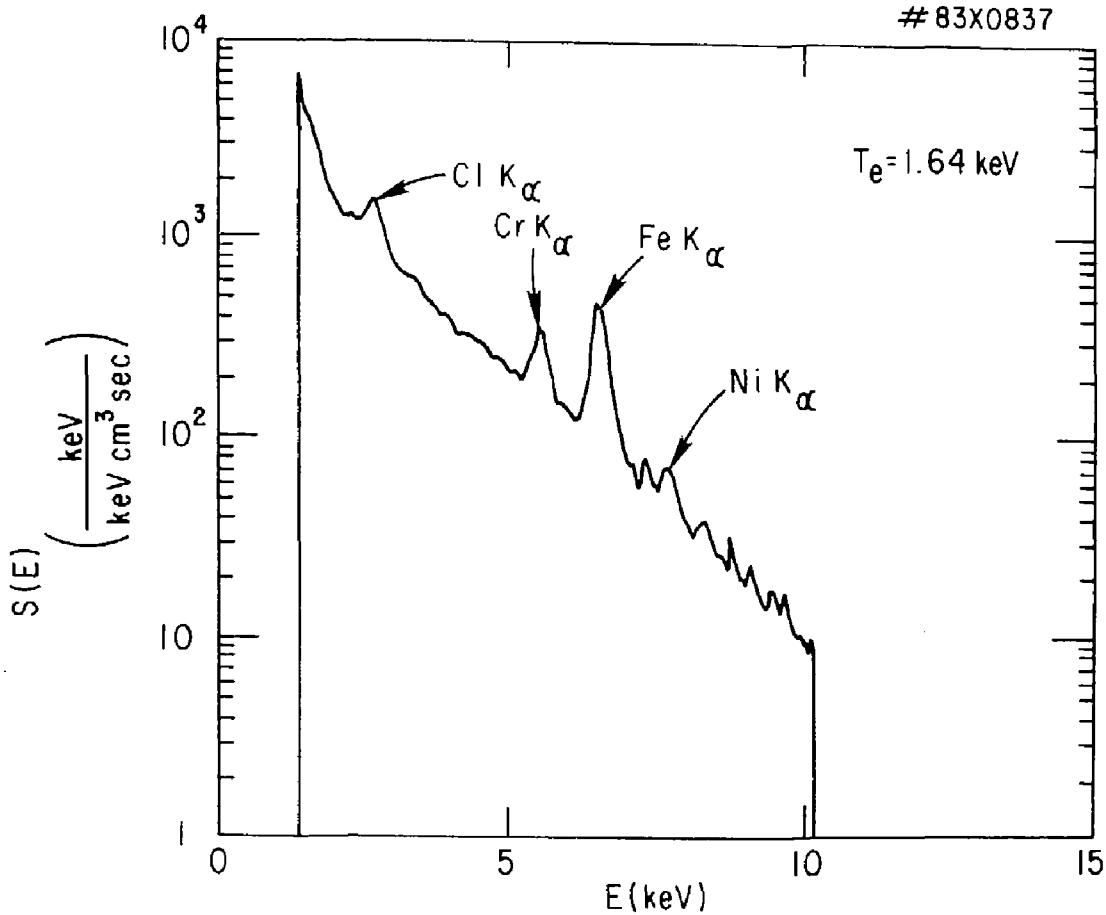
#83X0837
10^4
10^3
10^2
10
1
0
5
10
15
E(keV)
S(E) $\left(\frac{\text{keV}}{\text{keV cm}^3\text{ sec}}\right)$
Cl K_α
Cr K_α
Fe K_α
Ni K_α
T_e=1.64 keV

Fig. 10

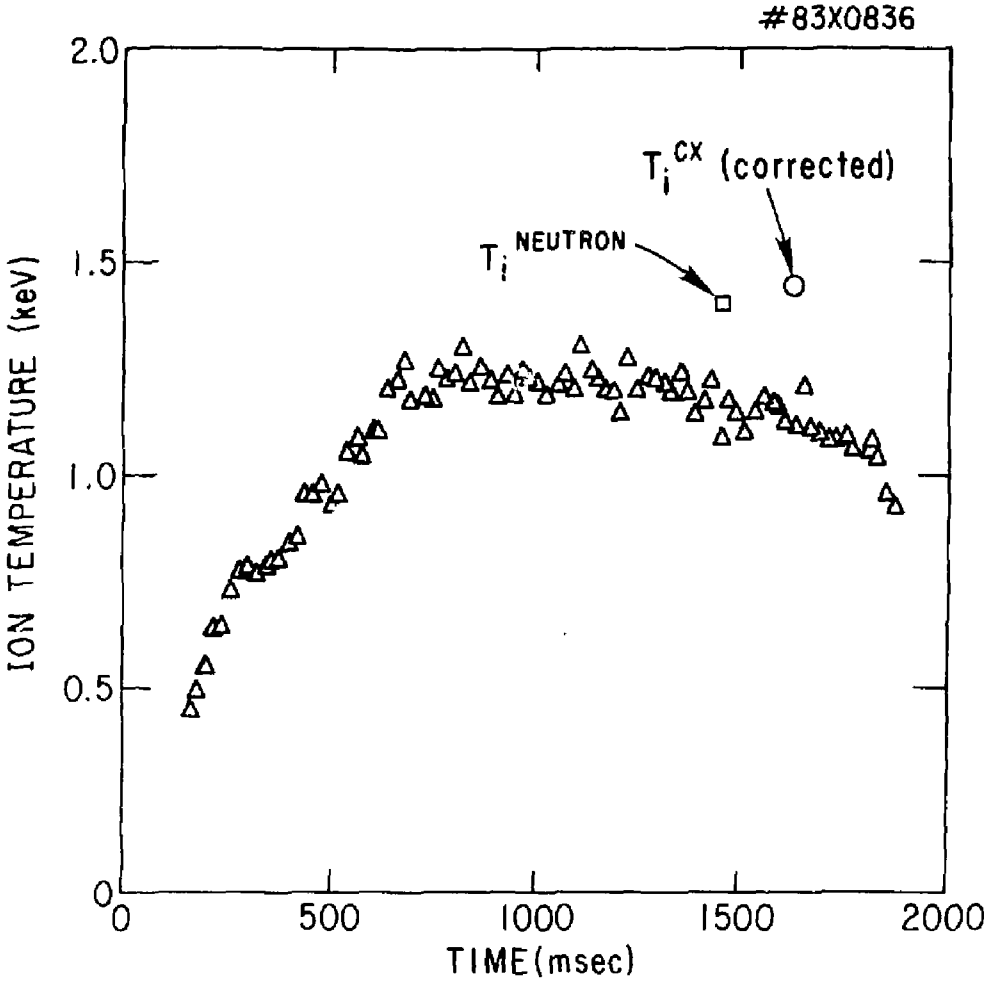
#83X0836
2.0
1.5
1.0
0.5
0
ION TEMPERATURE (keV)
T_i^{CX} (corrected)
$T_i^{NEUTRON}$
0
500
1000
1500
2000
TIME(msec)

Fig. 11

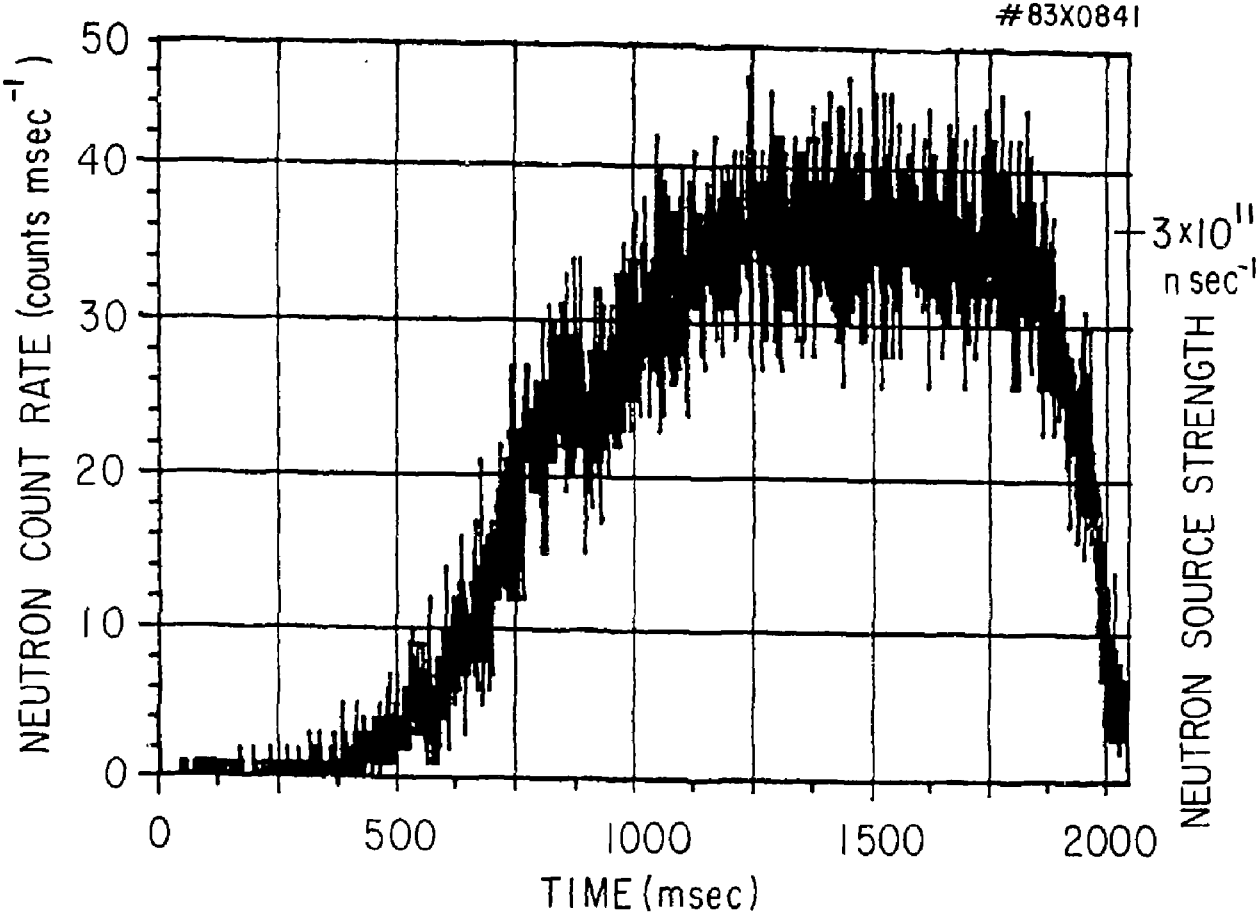
#83X0841
NEUTRON COUNT RATE (counts msec^{-1})
50
40
30
20
10
0
0
500
1000
1500
2000
TIME (msec)
3x10^{11}
n sec^{-1}
NEUTRON SOURCE STRENGTH

Fig. 12

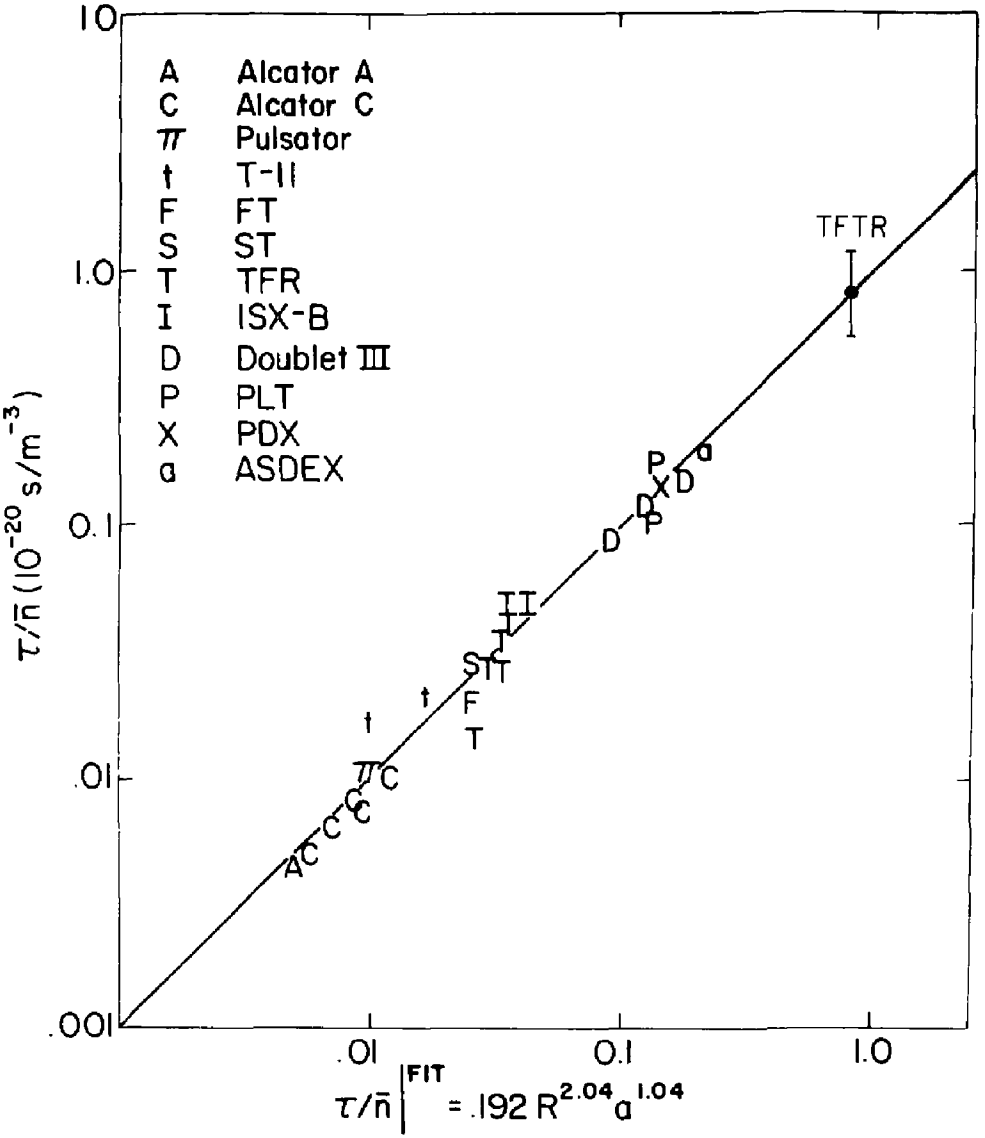
A Alcator A
C Alcator C
π Pulsator
t T-II
F FT
S ST
T TFR
I ISX-B
D Doublet III
P PLT
X PDX
a ASDEX
TFTR
10
1.0
0.1
.01
.001
.01
0.1
1.0
τ/n̄ (10^-20 s/m^-3)
τ/n̄|FIT = .192 R^2.04 a^1.04

Fig. 13a

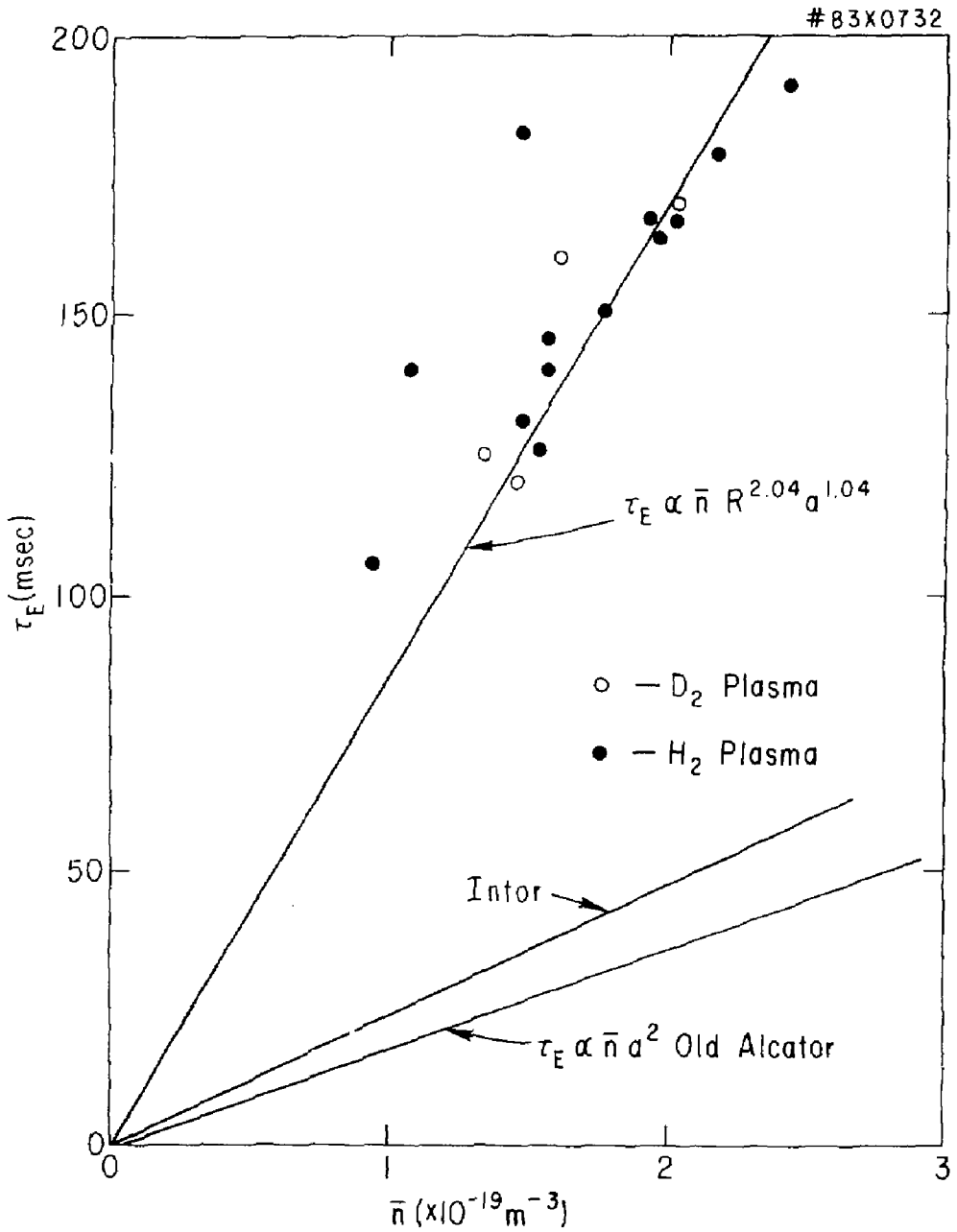
#83X0732
200
150
100
50
0
τ_E(msec)
0
1
2
3
$\bar{n}$ (x10^{-19}m^{-3})
$\tau_E \propto \bar{n}\, R^{2.04} a^{1.04}$
o — D_2 Plasma
• — H_2 Plasma
Intor
$\tau_E \propto \bar{n}\, a^2$ Old Alcator

Fig. 13b

EXTERNAL DISTRIBUTION IN ADDITION TO TIC UC-20

Plasma Res Lab, Austra Nat'l Univ, AUSTRALIA
Dr. Frank J. Paoloni, Univ of Wollongong, AUSTRALIA
Prof. I.R. Jones, Flinders Univ., AUSTRALIA
Prof. M.H. Brennan, Univ Sydney, AUSTRALIA
Prof. F. Cap, Inst Theo Phys, AUSTRIA
Prof. Frank Verheest, Inst theoretische, BELGIUM
Dr. C. Palumbo, Dg XII Fusion Prog, BELGIUM
Ecole Royale Militaire, Lab de Phys Plasmas, BELGIUM
Dr. P.H. Sakanaka, Univ Estadual, BRAZIL
Dr. C.R. James, Univ of Alberta, CANADA
Prof. J. Teichmann, Univ of Montreal, CANADA
Dr. H.M. Skarsgard, Univ of Saskatchewan, CANADA
Prof. S.R. Sreenivasan, University of Calgary, CANADA
Prof. Tudor W. Johnston, INRS-Energie, CANADA
Dr. Hannes Barnard, Univ British Columbia, CANADA
Dr. M.P. Bachynski, MPB Technologies, Inc., CANADA
Zhengwu Li, SW Inst Physics, CHINA
Library, Tsing Hua University, CHINA
Librarian, Institute of Physics, CHINA
Inst Plasma Phys, Academia Sinica, CHINA
Dr. Peter Lukac, Komenskeho Univ, CZECHOSLOVAKIA
The Librarian, Culham Laboratory, ENGLAND
Prof. Schatzman, Observatoire de Nice, FRANCE
J. Radet, CEN-BP6, FRANCE
AM Dupas Library, AM Dupas Library, FRANCE
Dr. Tom Mual, Academy Bibliographic, HONG KONG
Preprint Library, Cent Res Inst Phys, HUNGARY
Dr. S.K. Trehan, Panjab University, INDIA
Dr. Indra, Mohan Lal Das, Banaras Hindu Univ, INDIA
Dr. L.K. Chavda, South Gujarat Univ, INDIA
Dr. R.K. Chhajlani, Var Ruchi Marg, INDIA
P. Kaw, Physical Research Lab, INDIA
Dr. Phillip Rosenau, Israel Inst Tech, ISRAEL
Prof. S. Cuperman, Tel Aviv University, ISRAEL
Prof. G. Rostagni, Univ Di Padova, ITALY
Librarian, Int'l Ctr Theo Phys, ITALY
Miss Clelia De Palo, Assoc EURATOM-CNEN, ITALY
Biblioteca, del CNR EURATOM, ITALY
Dr. K. Yamato, Toshiba Res & Dev, JAPAN
Prof. M. Yoshikawa, JAERI, Tokai Res Est, JAPAN
Prof. T. Uchida, University of Tokyo, JAPAN
Research Info Center, Nagoya University, JAPAN
Prof. Kyoji Nishikawa, Univ of Hiroshima, JAPAN
Prof. Sigeru Mori, JAERI, JAPAN
Library, Kyoto University, JAPAN
Prof. Ichiro Kawakami, Nihon Univ, JAPAN
Prof. Satoshi Itoh, Kyushu University, JAPAN
Tech Info Division, Korea Atomic Energy, KOREA
Dr. R. England, Cividad Universiteria, MEXICO
Bibliotheek, Fom-Inst Voor Plasma, NETHERLANDS
Prof. B.S. Liley, University of Waikato, NEW ZEALAND
Dr. Suresh C. Sharma, Univ of Calabar, NIGERIA
Prof. J.A.C. Cabral, Inst Superior Tech, PORTUGAL
Dr. Octavian Petrus, ALI CUZA University, ROMANIA
Prof. M.A. Hellberg, University of Natal, SO AFRICA
Dr. Johan de Villiers, Atomic Energy Bd, SO AFRICA
Fusion Div, Library, JEN, SPAIN
Prof. Hans Wilhelmson, Chalmers Univ Tech, SWEDEN
Dr. Lennart Stenflo, University of UMEA, SWEDEN
Library, Royal Inst Tech, SWEDEN
Dr. Erik T. Karlson, Uppsala Universitet, SWEDEN
Centre de Recherchesen, Ecole Polytech Fed, SWITZERLAND
Dr. W.L. Weise, Nat'l Bur Stand, USA
Dr. W.M. Stacey, Georg Inst Tech, USA
Dr. S.T. Wu, Univ Alabama, USA
Prof. Norman L. Oleson, Univ S Florida, USA
Dr. Benjamin Ma, Iowa State Univ, USA
Prof. Magne Kristiansen, Texas Tech Univ, USA
Dr. Raymond Askew, Auburn Univ, USA
Dr. V.T. Tolok, Kharkov Phys Tech Ins, USSR
Dr. D.D. Ryutov, Siberian Acad Sci, USSR
Dr. G.A. Eliseev, Kurchatov Institute, USSR
Dr. V.A. Glukhikh, Inst Electro-Physical, USSR
Institute Gen. Physics, USSR
Prof. T.J. Boyd, Univ College N Wales, WALES
Dr. K. Schindler, Ruhr Universitat, W. GERMANY
Nuclear Res Estab, Julich Ltd, W. GERMANY
Librarian, Max-Planck Institut, W. GERMANY
Dr. H.J. Kaeppler, University Stuttgart, W. GERMANY
Bibliothek, Inst Plasmaforschung, W. GERMANY